



FDM Printed PLA/Coconut Wood Composite: Compression Characteristics and Parametric Optimization

Mahendran Samykano^{1,*}, Rajan Kumaresan¹, Reji Kumar Rajamony², Muhamad Mat Noor¹, Kumaran Kadirgama¹, Devarajan Ramasamy¹, Wan Sharuzi Wan Harun¹, Adarsh Kumar Pandey³, Avinash Maruti Badadhe⁴, Satesh Namasivayam⁵

¹ Faculty of Mechanical and Automotive Engineering Technology, Universiti Malaysia Pahang Al-Sultan Abdullah, 26600 Pekan, Pahang, Malaysia

² Institute of Sustainable Energy, Universiti Tenaga Nasional (National Energy University), 43000 Kajang, Selangor, Malaysia

³ Research Centre for Nano-Materials and Energy Technology (RCNMET), School of Engineering and Technology, Sunway University, Bandar Sunway, 47500 Petaling Jaya, Selangor, Malaysia

⁴ Department of Automation and Robotics, JSPM's Rajarshi Shahu College of Engineering, Pimpri-Chinchwad, Maharashtra 411033, India

⁵ Department of Engineering, Sunway University, Bandar Sunway, 47500 Petaling Jaya, Selangor, Malaysia

ARTICLE INFO

Article history:

Received 10 September 2024

Received in revised form 16 October 2024

Accepted 26 November 2024

Available online 31 December 2024

Keywords:

Fused deposition modelling; polylactic acid; coconut wood; biodegradable; response surface methodology

ABSTRACT

Fused Deposition Modelling (FDM) is a cost-effective technique within the realm of Additive Manufacturing (AM) that enables the fabrication of three-dimensional objects using thermoplastic and composite materials. FDM can generate complex parts with precise dimensions, which has helped the manufacturing industry. The biomedical industry uses wood particles; however, pure wood's mechanical properties are unknown. Coconut wood is biodegradable, heat and corrosion-resistant. The present study analyses the physical characteristics shown by Polylactic acid (PLA) and a tailored PLA/Ct.W composite. The compression properties of PLA and PLA/Ct.W specimens were investigated in accordance with ASTM standards (ASTM D695). Testing specimens were constructed using the FDM technique on PLA and PLA/Ct.W composite with different infill percentages (75%, 50% and 25%) and patterns (honeycomb, grid, concentric, rectilinear and octagram spiral). After that, the RSM is utilized to discover the parameter that has the largest effect on mechanical properties. Experimental results show that grid infill patterns with 75% infill percentages have the best compression properties. The weakest infill pattern is the octagram spiral. The RSM was employed to generate regression equations to optimize the properties of the PLA/Ct.W composite. It is suggested that the utilization of bonding agents can effectively augment the bonding between PLA and Coconut wood materials. Additionally, reducing the particle size of the coconut wood can further improve the overall quality of the product.

1. Introduction

The demand for increased flexibility and tailored products has been driving force behind the technological progress in additive manufacturing (AM) technology, commonly referred to as 3D

* Corresponding author.

E-mail address: mahendran@ump.edu.my

<https://doi.org/10.37934/armne.28.1.3046>

printing and recognized as rapid prototyping within the ASTM F42 technical committee [1]. This nomenclature is used to distinguish it from traditional production methods that involve subtracting manufacturing techniques. Initially, additive manufacturing techniques were solely employed for the purpose of conceptual visualization and validation [2]. The progress of the method has resulted in the creation of end-use elements and implements. The AM method involves the production of a component through layer-by-layer shaping, utilizing digital data proposed via computer-aided design (CAD) and computer-aided manufacturing (CAM) [3,4]. AM technology has significantly increased in modern years due to its capacity to accelerate the time-to-market of products compared to conventional procedures. Fused deposition modelling (FDM) has become widely recognized as a prominent AM technique, mostly due to its capacity to swiftly produce objects, its cost efficiency, its accessibility, its flexibility in material options and its capability to construct sophisticated components [5]. Crump obtained a patent for FDM in 1988 and subsequently established Stratasys in 1989. The primary system encompasses fundamental phases of additive manufacturing, albeit lacking the capability to produce intricate geometries [6]. Subsequently, a number of optimized sequences were unveiled, including FDM Titan, FDM Vantage, FDM Dimension and FDM Maxum, capable of fabricating intricate geometric designs [7].

The three-dimensional structure is fabricated on the build plate according to the CAD design through the utilization of thermoplastic filament in the FDM method. Upon completion of the first layer, the printing bed descends and subsequent layers are printed atop the preceding layer, thereby perpetuating the process [8,9]. ABS and PLA are commonly utilized materials in Fused Deposition Modelling (FDM) due to their favourable thermal and rheological characteristics, which facilitate the production of parts. The literature suggests that the processing parameters plays a critical role in deciding the quality and behaviour of the output product [3,10,11]. Various processing parameters were employed in FDM process, including infill pattern, layer thickness, printing speed, infill density, raster angle, build orientation, raster width and bed temperature [12,13]. The anisotropic properties of FDM-manufactured parts are significantly impacted negatively. Numerous scholars have conducted research on how FDM parameters affect mechanical characteristics. Polylactic acid (PLA) is a well-known biopolymer with applications in medicine, particularly in tissue regeneration. Instead of metal, it can be PLA because it is biocompatible, biodegradable and bioresorbable [14,15]. It has some restrictions, however, because of its hydrophobicity, brittleness and subpar mechanical properties. Many polymeric materials are accessible, but it's been exciting to see what may be created by combining different polymer composites. These are the outcome of the process' inherent flaws, which provide subpar raw materials. To get over this restriction and extend polymers' usefulness, we need to see increased demand for new, higher-performance composite materials. There has been a rise in the use of bio-composite filaments formulated with a variety of fillers, most notably PLA combined with other bio-based materials [10,16]. The study examined the impact of different infill orientations on distinct sample properties of FDM in the context of wood/PLA composites [17]. The authors documented a correlation between the orientation of the infill material and the mechanical properties of the sample under investigation. Furthermore, Sun *et al.*, [18] examined the mechanical behaviour and biodegradability of composites made from polylactic acid (PLA) and wood filler fabricated using fused deposition modelling (FDM) with varying infill settings. According to their report, the incorporation of 30-weight per cent wood fibre in PLA-based filaments used for 3D printing results in composites that demonstrate resistance to biodegradation by typical decay fungi.

The utilization of coconut wood particles has been identified as a promising component for composite filaments. The incorporation of coconut wood particles into polylactic acid (PLA) is achieved by blending the particles in a powdered state, followed by extrusion to obtain a filamentous

form. Coconut wood exhibits water resistance, providing an added benefit. Coconut wood-PLA composites (Ct. W-PLA) have potential applications in construction and biomedical fields, particularly in tissue remodelling. They offer a viable alternative to metal alloys in orthopaedics due to biomedical concerns associated with metal. The filament application procedure in FDM production may disrupt the sustainable material flow. This matter has led several research teams to develop a new composite filament possessing superior mechanical properties compared to PLA. Selecting optimal printing parameters and filament materials is crucial for achieving superior mechanical properties in the FDM process. This study seeks to ascertain if modifications to printing parameters (infill % (75%, 50% and 25%) and infill structures (rectilinear, grid, honeycomb, concentric and octagram spiral)) can impact the mechanical properties of composite filament (PLA/Ct.W).






2. Methodology

The PLA and Ct.W filled PLA composite filament utilized in this research project was obtained from Form Futura. The PLA filament's operational temperature ranges from 180 to 210 °C, while the composite's operating temperature ranges from 200 to 240 °C. The composite material comprising wood materials and PLA filament has a composition of 40% and 60%, respectively. The PLA and coconut-PLA with a standard dia of 1.75 mm (± 0.04 mm) is utilized as the standard. The FDM printer meets the minimum requirements for printing specimens for mechanical testing. SolidWorks has been used for designing the specimen. The specimens have been manufactured in compliance with the ASTM guidelines for mechanical evaluation. The model is transferred to the slicing software through the use of a USB drive. The software enables the visualization of STL files on a platform by providing G-code. The slicing software is utilized to customize printing parameters based on specific requirements. The parameters under study are the changes in infiltration patterns and percentages. G-code making follows parameter configuration. Ensuring a consistent temperature of the nozzle and heated bed is imperative during printing procedure. Once printing process is completed, the finalized product undergoes rigorous evaluation in the mechanical testing laboratory. ASTM D695 is the standard for compression testing. The compression test utilized a cylindrical specimen with a diameter of 12.7 mm. The INSTRON 3367 machine is utilized for compression testing, similar to the tensile testing machine. The examination follows the ASTM D695 standard and involves testing a 25.4mm length at a rate of 1.3 ± 0.03 mm/min. The various parameters that are used in this study are shown in Table 1 and the various infill patterns are displayed in Table 2.

Table 1
Process parameters for the study

No	Parameters	Constants
1	Layer height	0.30 mm
3	Nozzle diameter	0.4 mm
4	Diameter of the filament	1.75 mm
5	Temperature of the nozzle	200 °C
6	Speed of printing	30 mm/min
7	Temperature of the bed	60 °C
8	Raster angle	0°

Table 2
Various infill patterns

Concentric	
Honeycomb	
Rectilinear	
Octagram-spiral	
Grid	

3. Results

3.1 Compression Test

A sample's compression strength indicates its ability to resist the gradual application of compressive stress or loads, resulting in a reduction in height or size. The application of compressive force is employed in order to ascertain the modulus. In order to ascertain the compression modulus, compressive stress can be computed by the ratio of the highest load obtained from the raw data to the sectional area of the printed sample. The aforementioned approach is employed for assessing the rigidity of a substance. The compressive behaviour of the pure PLA is indicated in Table 3 and PLA/ Coconut wood composite in Table 4.

Table 3

Compressive properties of PLA sample with respect to different infill percentages and patterns

Infill pattern	Infill percentage (%)	Compression strength (MPa)	Compression modulus (GPa)
Octagram Spiral	25	25.89	0.43
Rectilinear	25	24.12	0.48
Honeycomb	25	24.21	0.47
Grid	25	26.45	0.48
Concentric	25	25.43	0.42
Octagram Spiral	50	31.45	0.70
Rectilinear	50	29.28	0.54
Honeycomb	50	30.74	0.64
Grid	50	37.09	0.84
Concentric	50	34.21	0.77
Octagram Spiral	75	37.13	0.95
Rectilinear	75	33.90	0.79
Honeycomb	75	35.20	0.84
Grid	75	41.64	1.33
Concentric	75	39.53	1.36

Table 4

Compressive performance of PLA/Ct.W sample with respect to different infill percentages and patterns

Infill pattern	Infill percentage (%)	Compression strength (MPa)	Compression modulus (GPa)
Octagram Spiral	25	5.29	0.08
Rectilinear	25	4.51	0.06
Honeycomb	25	4.57	0.06
Grid	25	6.47	0.09
Concentric	25	5.58	0.07
Octagram Spiral	50	9.06	0.12
Rectilinear	50	7.43	0.10
Honeycomb	50	8.23	0.11
Grid	50	10.52	0.14
Concentric	50	9.19	0.13
Octagram Spiral	75	12.43	0.17
Rectilinear	75	12.20	0.16
Honeycomb	75	12.40	0.16
Grid	75	13.88	0.19
Concentric	75	13.37	0.17

3.1.1 Compressive strength

The results obtained with the compression test using the PLA and PLA/Ct.W Composite filament are tabulated in Table 3 and Table 4. The maximum compressive strength of PLA is 41.64 MPa, achieved using a Honeycomb pattern with 75% infill density. After that, the PLA sample with the rectilinear infill pattern and a 25% infill % has a compressive strength of 24.12 MPa, making it the material with the lowest strength. Table 4 and Figure 1 for composite filament (PLA/Ct.W), the highest compressive strength of 13.88 MPa was noted for the Honeycomb structure with a 75% infill percentage. Since more surfaces were made, a higher value may have been reached, which could mean that more energy was used [19]. The compression strength of the 75%, 50% and 25% infill percentages were ranked in descending order, with the highest value observed in the 75% infill. Honeycomb specimens exhibit the highest compressive strength, followed by concentric, Grid, Octagram spiral and rectilinear infill patterns. The observed outcomes can be rationalized based on the inherent characteristic of 2D infill patterns, wherein the material is consistently deposited in a singular direction. Consequently, these patterns exhibit enhanced stress resistance, particularly in

the direction of deposition (namely, compression), compared to other directions. The Honeycomb pattern recommends having the best compressive strength value for both PLA and Composite filament. However, the PLA sample has better compressive strength than the composite filament. Because coconut wood and PLA do not stick together well, the composite filament may not be strong when it comes to compression. To improve the behaviour even more, it is suggested that a suitable or extra bonding agent be used. Annealing the composite filament could be a potential solution for minimizing the residual stress and improving mechanical strength.

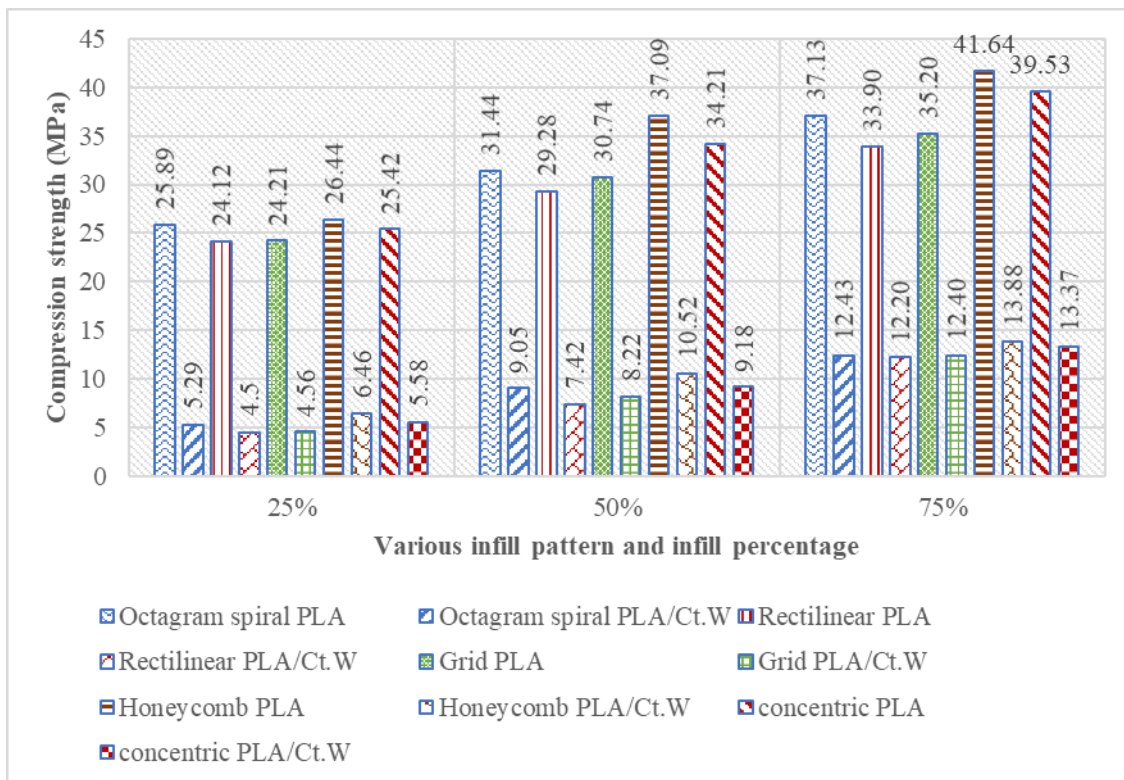


Fig. 1. Experimental value of compressive strength respect to different infill patterns

3.1.2 Compressive modulus

Figure 2 and Table 3 found that 75% infill with a concentric infill pattern achieves 1.36 GPa compressive modulus for PLA. At 25% concentric infill, the PLA achieves the lowest compressive modulus by 0.42 GPa. Table 4 and Figure 2 show that the PLA/Ct.W specimen's maximum compression modulus is 0.19 GPa at 75% infill with a honeycomb design. This issue can be attributed to the large size of the cells and their irregular shape [20]. Figure 2 shows that the specimen's compression modulus increases with increasing infill percentage. Also, the PLA/Ct.W compressive modulus is lower than pure PLA. However, the Honeycomb-patterned specimens had the greatest compressive modulus for both filaments except for the composite filament of 75% infill. Still, the value is almost very close to the concentric pattern. It appears that the Honeycomb pattern was able to withstand the highest compressive strength due to the effective layer contacts in that direction. The PLA/Ct.W compressive modulus was found to be lower due to the poor interlayer bond between the PLA and coconut wood. To improve the behaviour even more, it is suggested that a suitable or extra bonding agent be used.

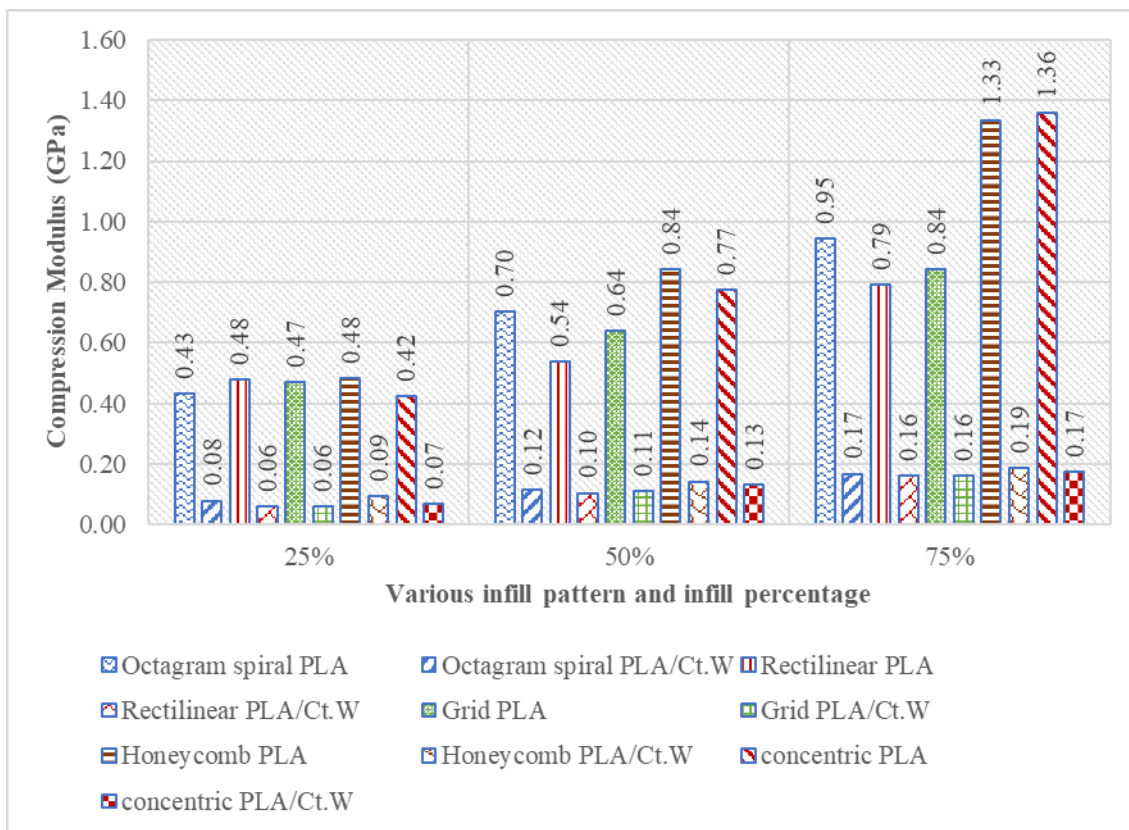


Fig. 2. Experimental values of compressive strength with respect to different infill patterns

3.2 Statistical Analysis of the Compression Properties (PLA/CW Filament)

3.2.1 Statistical analysis of compression strength

From Table 5, infill patterns account for around 52.18% and infill percentages for 41.07% of the total. It demonstrates that both infill percentage and infill design significantly influence compression strength. Also, the two-way interaction is also a very important parameter. The value of R^2 is 99.35%, which means that the better model fits the data. Further, the relationship's importance is shown by the adjusted R^2 , which is equal to 97.72%. Because the adjusted R^2 is larger, the suggested mathematical model reveals more information about the link between the attributes and the response. On the other hand, the predicted R^2 shows that the model is 93.52% accurate at making predictions. The model's P-value is 0.000, indicating statistical significance at a significance level of 0.05. Based on the obtained data, it may be inferred that the model exhibits statistical significance.

Table 5
 Compression strength ANOVA table for PLA/Ct.W

Source	DF	Contribution	Adj SS	Adj MS	F-value	P-value
Model	10	99.67%	0.032369	0.003237	122.14	0.000
Linear	5	93.25%	0.030284	0.006057	228.54	0.000
Infill %	1	41.07%	0.013338	0.013338	503.31	0.000
Infill Pattern	4	52.18%	0.016945	0.004236	159.85	0.000
Square	1	0.99%	0.000320	0.000320	12.07	0.025
Infill %*Infill %	1	0.99%	0.000320	0.000320	12.07	0.025
2-Way Interaction	4	5.44%	0.001765	0.000441	16.65	0.009
Infill %*Infill Pattern	4	5.44%	0.001765	0.000441	16.65	0.009
Error	4	0.33%	0.000106	0.000027		
Total	14	100.00%				

R² = 99.35%
 R² –adjusted = 97.72%
 R² –predicted = 93.52%

The generated model through this analysis is displayed in Table 6.

Table 6
 Compression strength regression equation for PLA/Ct.W

Infill Pattern	Regression equation
1	0.0875 - 0.000899 Infill % + 0.000016 Infill %*Infill %
2	0.0796 - 0.000558 Infill % + 0.000016 Infill %*Infill %
3	0.0867 + 0.000162 Infill % + 0.000016 Infill %*Infill %
4	0.0753 + 0.000250 Infill % + 0.000016 Infill %*Infill %
5	0.1110 + 0.000511 Infill % + 0.000016 Infill %*Infill %

According to Figure 3, the mean effect plot directs an increase in infill percentage, resulting in a corresponding increase in compression strength.

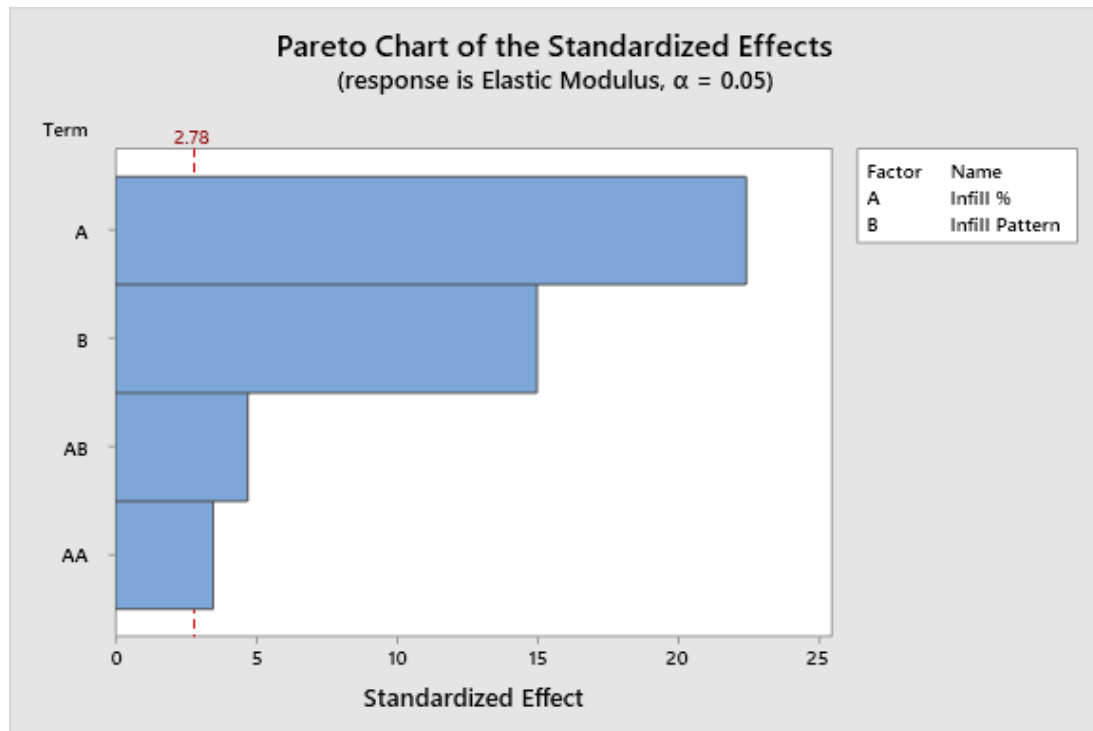


Fig. 3. Compression strength pareto chart for PLA/Ct.W

According to Figure 4, the data points are more closely aligned with normal line. This shows that the prediction was accurate.

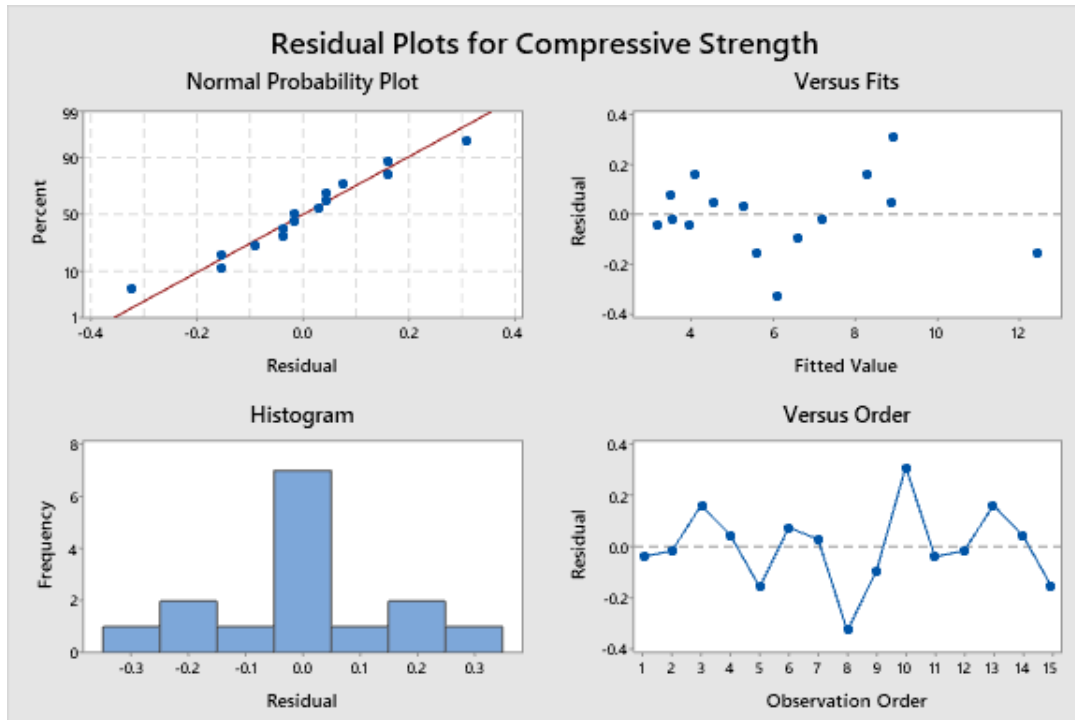


Fig. 4. Compression strength residual plot for PLA/Ct.W

Figure 5 and Figure 6 exhibit the effect and interaction plot of the various parameters. It clearly demonstrates the concentric pattern and 75% of infill % achieves the extreme properties.

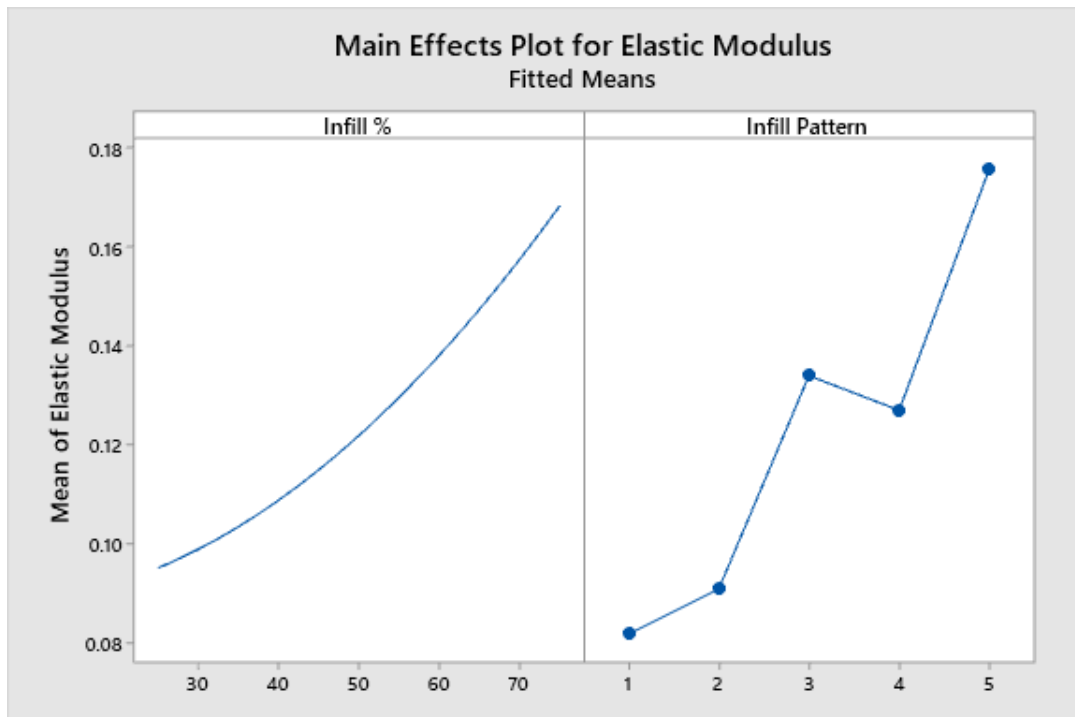


Fig. 5. Compression vs infill % and infill pattern of PLA/Ct.W

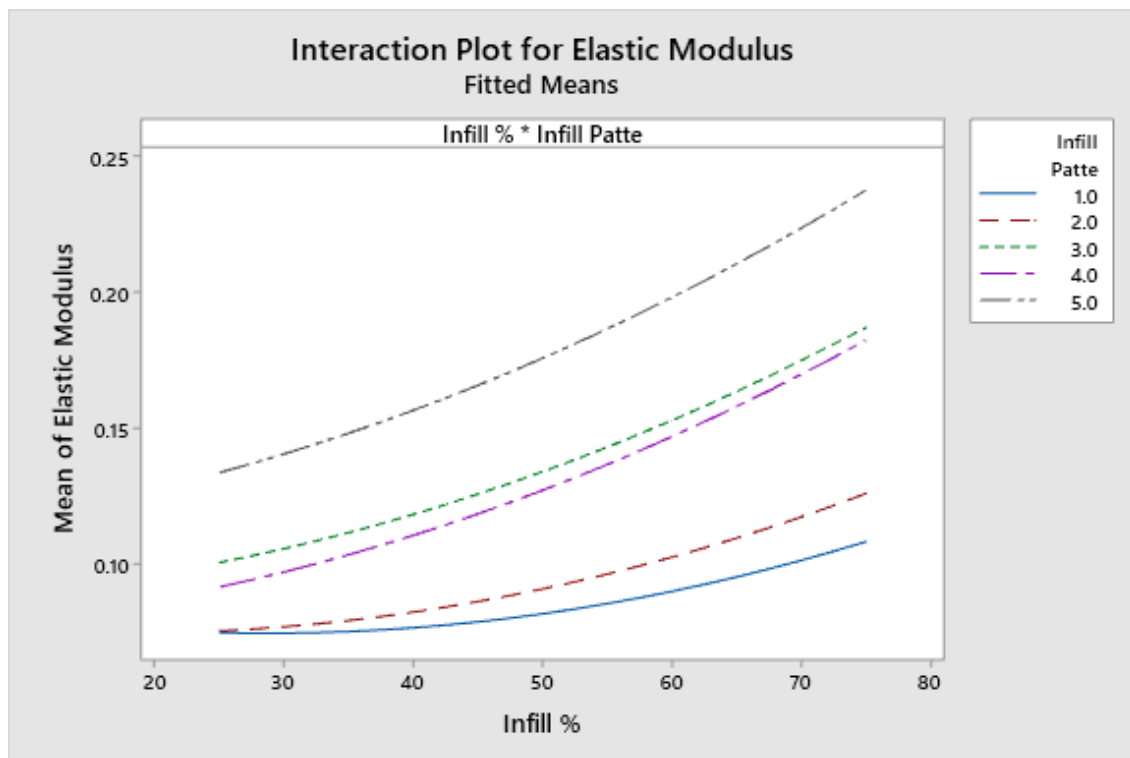


Fig. 6. Compression strength interaction plot for PLA/Ct.W

3.2.1.1 Comparison of experimental and predicted compression strength

The experimentally determined compression strength data are compared to theoretical explanations, as illustrated in Table 7 and Figure 7. The error between practical and theoretical values shows a very small difference. The mathematical model for compression strength exhibits a range of computed errors, spanning from a minimum of 0.20% to a maximum of 5.79% and a mean value of 2.05%. As a result, the mathematical model is highly recommended for estimating or forecasting compression strength.

Table 7
 Error percentage in compression modulus of PLA/Ct.W

Infill pattern	Infill percentage (%)	Experimental compression strength (MPa)	Predicted compression strength (MPa)	Error (%)
Octagram Spiral	25	9.23	3.16	2.33
Rectilinear	25	3.90	3.53	5.79
Concentric	25	7.15	4.08	0.52
Grid	25	8.43	4.51	2.68
Concentric	25	8.95	5.57	0.62
Octagram Spiral	50	12.31	3.45	2.89
Rectilinear	50	7.36	5.25	6.22
Concentric	50	8.15	6.07	0.57
Grid	50	10.42	6.61	3.51
Concentric	50	9.10	8.91	0.74
Octagram Spiral	75	12.31	3.94	1.01
Rectilinear	75	12.08	7.17	2.07
Concentric	75	12.28	8.27	0.20
Grid	75	13.74	8.90	1.26
Concentric	75	13.24	12.46	0.27
Total Error (%) = 2.05				

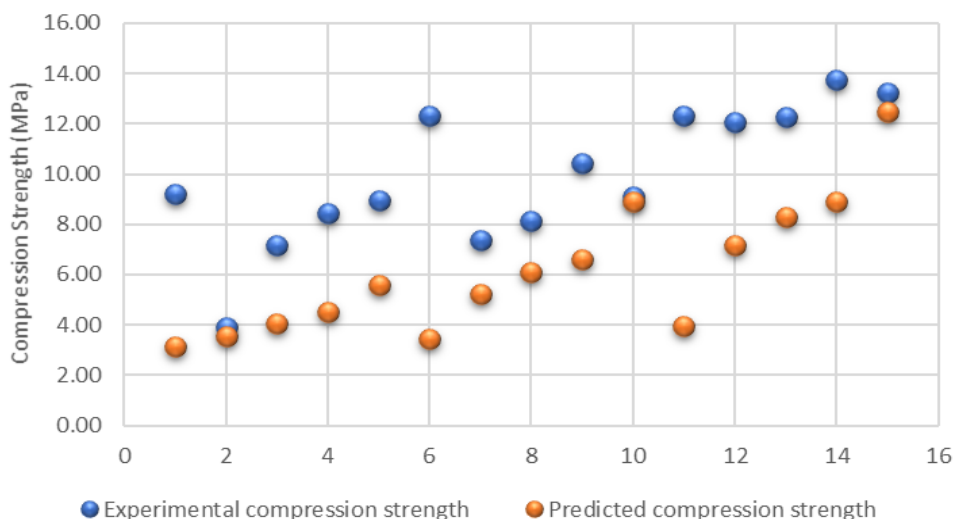


Fig. 7. Experimental and predicted results of compression modulus for PLA/Ct.W

3.2.2 Statistical analysis of compression modulus

The examination of Table 8 indicates that both the infill % and infill pattern substantially impacts the statistical analysis. This is substantiated by the P-values of 0.000 and 0.000, correspondingly, both of which fall below the intended significance level of 0.05. Also, second-order component of the infill pattern, the infill % and their interplay do not have an effect on the mechanical performance.

Table 8
 Compression modulus ANOVA table for PLA/Ct.W

Source	DF	Contribution	Adj SS	Adj MS	F-value	P-value
Model	10	99.67%	0.032369	0.003237	122.14	0.000
Linear	5	93.25%	0.030284	0.006057	228.54	0.000
Infill %	1	41.07%	0.013338	0.013338	503.31	0.000
Infill Pattern	4	52.18%	0.016945	0.004236	159.85	0.000
Square	1	0.99%	0.000320	0.000320	12.07	0.025
Infill %*Infill %	1	0.99%	0.000320	0.000320	12.07	0.025
2-Way Interaction	4	5.44%	0.001765	0.000441	16.65	0.009
Infill %*Infill Pattern	4	5.44%	0.001765	0.000441	16.65	0.009
Error	4	0.33%	0.000106	0.000027		
Total	14	100.00%				

$R^2 = 99.35\%$
 $R^2 \text{ -adjusted} = 97.72\%$
 $R^2 \text{ -predicted} = 93.52\%$

In Figure 8, the length of each bar corresponds to the absolute amount of the projected results at a 95% assurance level. This representation allows for a visual comparison of the projected effects. The impact of various patterns and infill % on the compression modulus is demonstrated in Figure 10. Table 8 demonstrates that the R^2 value is directly proportional to the degree of fit between the model and the data. Specifically, the R^2 value is 99.35%, indicating a high level of accuracy in the model's ability to explain the variability observed in the data. The user states that the adjusted R^2 is 97.72%, indicating a high level of significance in the association being studied. The adjusted R^2 value signifies that the proposed mathematical model aptly accounts for the relationship between the attributes and the response. The user has provided information regarding the anticipated R^2 value, which measures the accuracy of the model in expected outcomes. The value of R^2 is expected to be

93.52%. The model's statistical significance is substantiated by the P-value of 0.000, which falls below the preset alpha level of 0.05. From the analysis, it may be deduced that the model exhibits statistical significance.

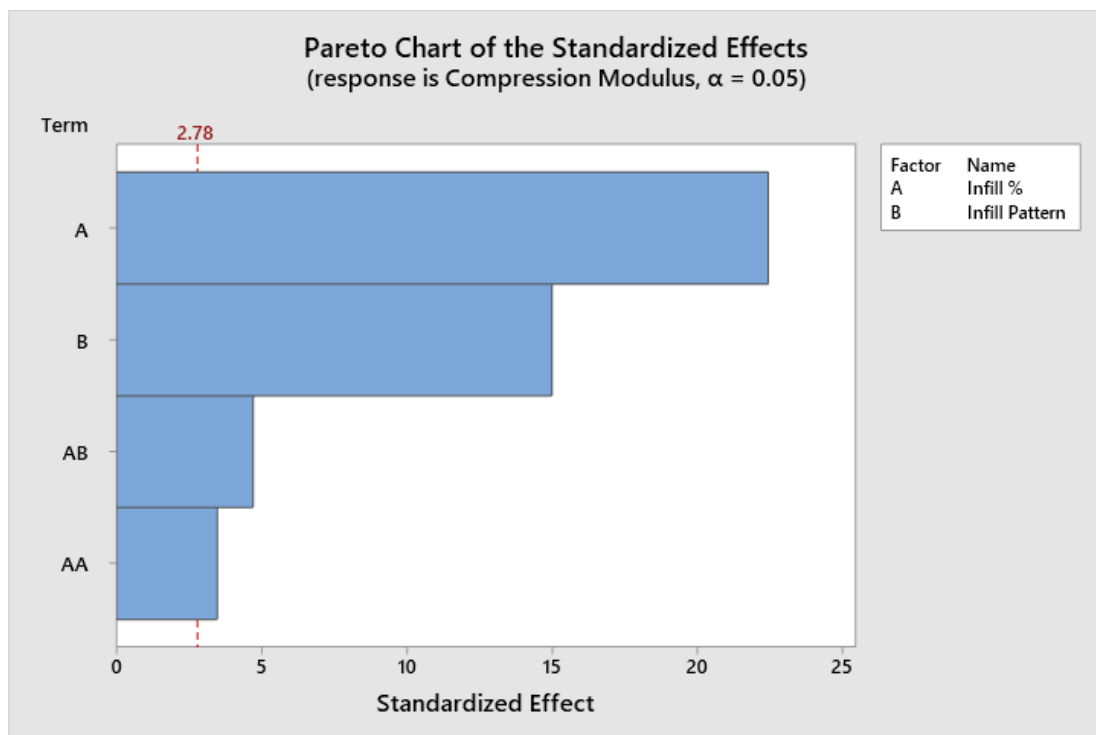


Fig. 8. Compression modulus pareto chart for PLA/Ct.W

Table 9 displays the model that was generated as a result of the investigation. Each infill scheme has a distinct equation to model the compression modulus.

Table 9

Compression modulus regression equation for PLA/Ct.W

Infill Pattern	Regression equation
1	$0.0875 - 0.000899 \text{ Infill \%} + 0.000016 \text{ Infill \%} * \text{Infill \%}$
2	$0.0796 - 0.000558 \text{ Infill \%} + 0.000016 \text{ Infill \%} * \text{Infill \%}$
3	$0.0867 + 0.000162 \text{ Infill \%} + 0.000016 \text{ Infill \%} * \text{Infill \%}$
4	$0.0753 + 0.000250 \text{ Infill \%} + 0.000016 \text{ Infill \%} * \text{Infill \%}$
5	$0.1110 + 0.000511 \text{ Infill \%} + 0.000016 \text{ Infill \%} * \text{Infill \%}$

The normal probability distribution indicates that the data points are closely clustered around the normal curve. The residual plot for the UTS is shown in Figure 9.

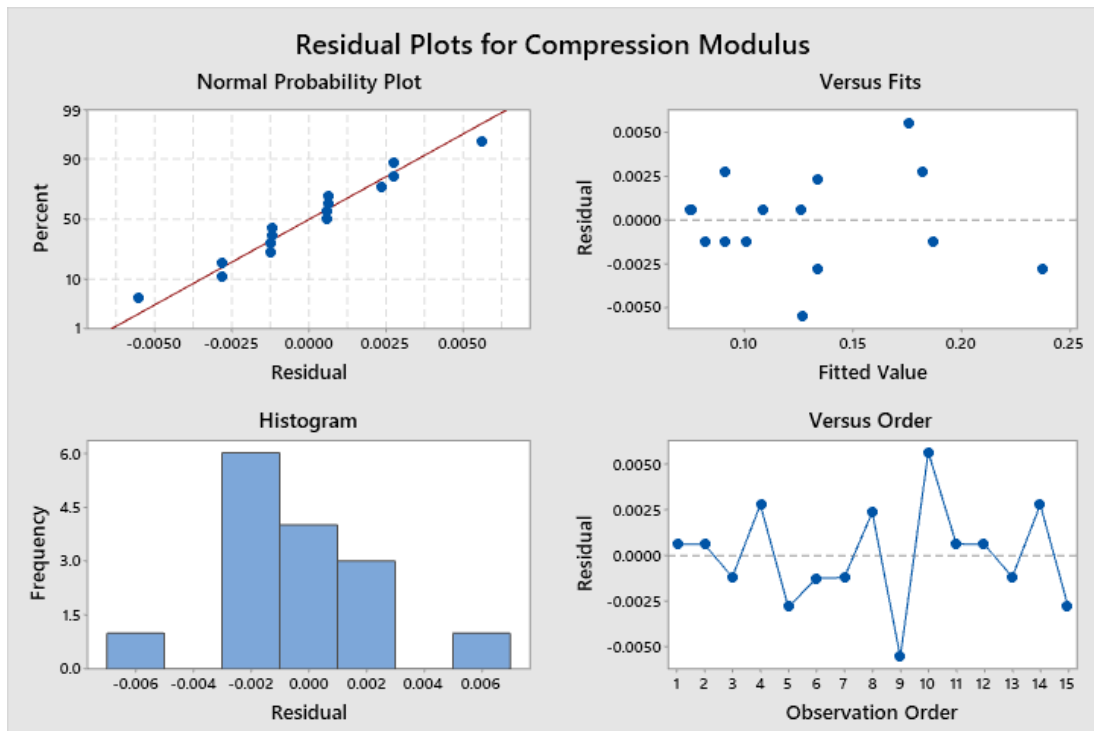


Fig. 9. Compression modulus residual plot for PLA/Ct.W

This demonstrates how accurate the anticipated model is. The effect and interaction plot of the parameters on the compression modulus is shown in Figure 10 and Figure 11. Based on the available data, it appears the concentric pattern with infill percentage of 75% yields the most favourable PLA/Ct.W physical characteristics.

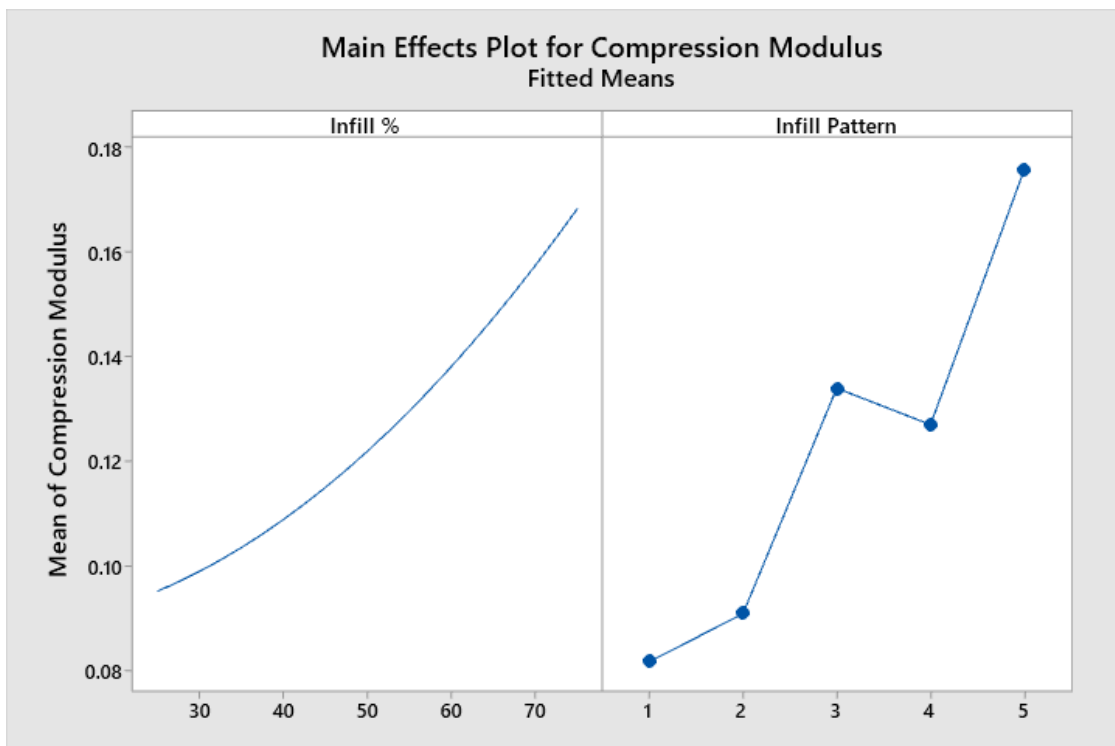


Fig. 10. Compression strength vs infill % and pattern for (PLA/Ct.W)

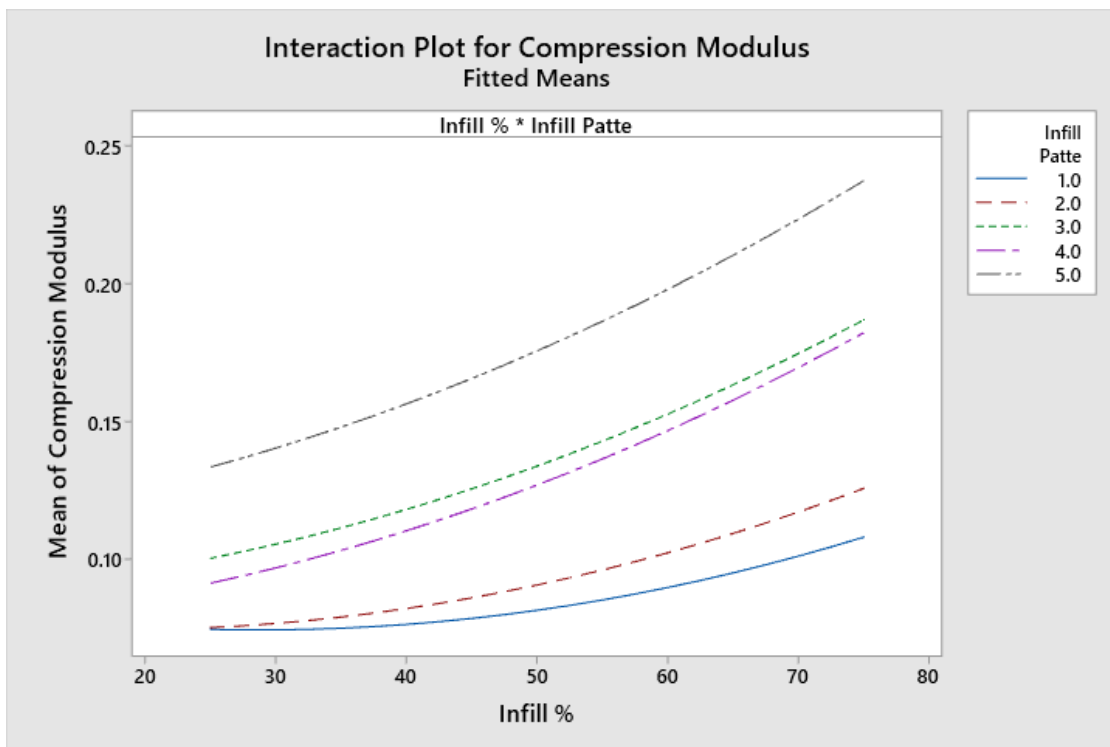


Fig. 11. Compression strength interaction plot for PLA/Ct.W

3.2.2.1 Comparison of experimental and predicted compression modulus

As shown in Table 10 and Figure 12, a comparison between the experimentally acquired compression modulus data and theoretical techniques is made. The calculated average error is minimal when comparing practical and theoretical values. The statistical data pertaining to the computed error associated with the mathematical model of compression strength is presented

Table 10
 Error percentage of compression strength for PLA/Ct.W

Infill pattern	Infill percentage (%)	Average experimental flexural modulus (GPa)	Predicted flexural modulus (GPa)	Error (%)
Octagram Spiral	25	0.08	0.07	3.69
Rectilinear	25	0.08	0.08	3.63
Concentric	25	0.10	0.10	0.00
Grid	25	0.09	0.09	1.19
Concentric	25	0.13	0.13	4.84
Octagram Spiral	50	0.08	0.08	4.52
Rectilinear	50	0.09	0.09	3.81
Concentric	50	0.14	0.13	0.09
Grid	50	0.12	0.13	1.73
Concentric	50	0.18	0.18	5.83
Octagram Spiral	75	0.11	0.11	1.71
Rectilinear	75	0.13	0.13	1.33
Concentric	75	0.19	0.19	0.00
Grid	75	0.19	0.18	1.37
Concentric	75	0.23	0.24	1.99
Total Error (%) = 2.38				

The average error is 2.38 per cent, with the minimum mistake recorded as 0.00 per cent and the maximum error recorded as 5.83 per cent. For this reason, the mathematical model is strongly recommended for estimating or forecasting compression strength.

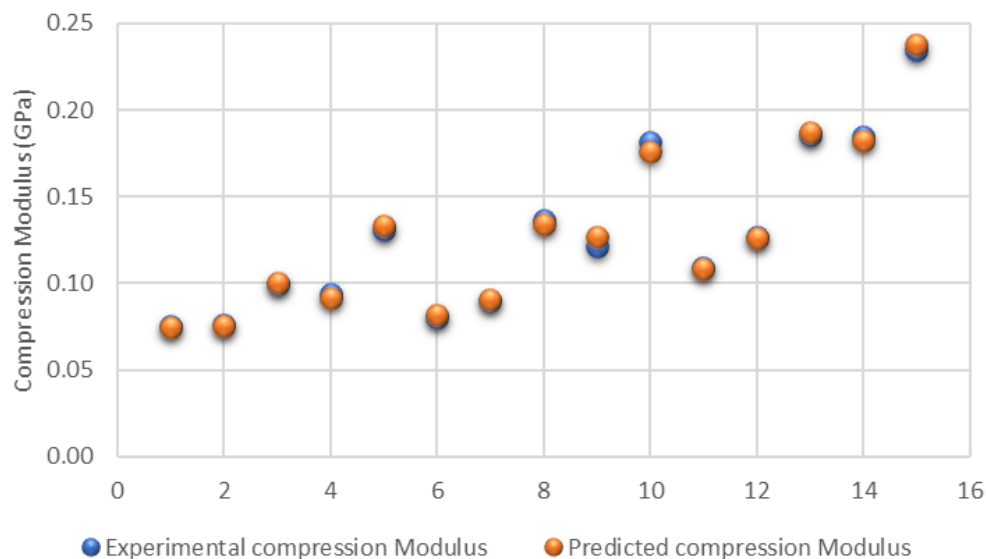


Fig. 12. Experimental and predicted results of compression strength for PLA/Ct.W

4. Conclusions

The current research spotlights PLA's production and mechanical characteristics and tailor-made PLA/Ct.W bio composite. The compressive properties of the PLA and PLA/Ct.W materials that were developed were analysed at different infill percentages. RSM was used to evaluate the expected mechanical properties. The compression test results demonstrate that both the infill density and pattern significantly inspire the compression modulus and strength. The implementation of the honeycomb and concentric pattern and infill density with 75% yields the best compression properties of 41.64 MPa and 1.36 GPa. Also, in the PLA/ Ct. W composite of the Honeycomb infill pattern with 75% infill density obtained the maximum properties of 13.88 MPa and 0.19 GPa. From this, the compressive performance of the PLA is higher than the PLA/ Ct. W. The mathematical models derived from Response Surface Methodology (RSM) indicate that the compression strength and compression modulus are significantly influenced by both the infill % and infill pattern. The application of the honeycomb infill design in combination with a 75% infill ratio yields the most optimal compression characteristics. The model that has been created demonstrates a notable level of reliability in its capacity to accurately predict the properties of interest. This is evident as the disparity between the predicted value and the corresponding experimental value is observed to be less than 5.0%. The observed deviation between the measured and expected values is 3.25% for the compressive strength and 2.56% for the compressive modulus. The R^2 value of the model is more than 95%, which shows the developed model fits the data. The outcome of the compressive test of PLA/ Ct.W-based 3D printed composite samples indicated that the compression caused the Ct.W particles to be squeezed, resulting in the creation of a slippery surface. This, in turn, caused the Ct.W particles to move and leave a wear mark when subjected to a load. The presence of a significant amount of Ct.W, specifically 40%, in the PLA/Ct.W matrix resulted in agglomeration. Consequently, this resulted in the formation of voids with in the inter-layer bonding, ultimately causing a reduction in the compressive strength of the Ct.W/PLA composite.

Acknowledgement

The authors express their gratitude to Universiti Malaysia Pahang Al-Sultan Abdullah, Malaysia, for the financial support and resources provided through International Grant UIC211506, which enabled the successful completion of this study.

References

- [1] Rajan, Kumaresan, Mahendran Samykan, Kumaran Kadirgama, Wan Sharuzi Wan Harun and Md Mustafizur Rahman. "Fused deposition modeling: process, materials, parameters, properties and applications." *The International Journal of Advanced Manufacturing Technology* 120, no. 3 (2022): 1531-1570. <https://doi.org/10.1007/s00170-022-08860-7>
- [2] Kananathan, J., K. Rajan, M. Samykan, K. Kadirgama, K. Moorthy and M. M. Rahman. "Preliminary Tensile Investigation of FDM Printed PLA/Coconut Wood Composite." In *International Conference on Mechanical Engineering Research*, pp. 339-350. Singapore: Springer Nature Singapore, 2021. https://doi.org/10.1007/978-981-19-1577-2_26
- [3] Wankhede, Vishal, Darshit Jagetiya, Akshata Joshi and Rakesh Chaudhari. "Experimental investigation of FDM process parameters using Taguchi analysis." *Materials Today: Proceedings* 27 (2020): 2117-2120. <https://doi.org/10.1016/j.matpr.2019.09.078>
- [4] Egiziano, Luigi, Patrizia Lamberti, Giovanni Spinelli, Vincenzo Tucci, Rumiana Kotsilkova, Sonia Tabakova, Evgeni Ivanov, Clara Silvestre and Rosa Di Maio. "Morphological, rheological and electrical study of PLA reinforced with carbon-based fillers for 3D printing applications." In *AIP Conference Proceedings*, vol. 1981, no. 1. AIP Publishing, 2018. <https://doi.org/10.1063/1.5046014>
- [5] Farah, Shady, Daniel G. Anderson and Robert Langer. "Physical and mechanical properties of PLA and their functions in widespread applications—A comprehensive review." *Advanced drug delivery reviews* 107 (2016): 367-392. <https://doi.org/10.1016/j.addr.2016.06.012>
- [6] Ahn, Sung-Hoon, Michael Montero, Dan Odell, Shad Roundy and Paul K. Wright. "Anisotropic material properties of fused deposition modeling ABS." *Rapid prototyping journal* 8, no. 4 (2002): 248-257. <https://doi.org/10.1108/13552540210441166>
- [7] Hiemenz, Joe. "Additive manufacturing trends in aerospace." *White Paper, Stratasys, USA* (2014): 1-11.
- [8] Kumaresan, Rajan, Mahendran Samykan, Kumaran Kadirgama, Devarajan Ramasamy, Ngui Wai Keng and Adarsh Kumar Pandey. "3D printing technology for thermal application: a brief review." *Journal of Advanced Research in Fluid Mechanics and Thermal Sciences* 83, no. 2 (2021): 84-97. <https://doi.org/10.37934/arfmts.83.2.8497>
- [9] Niu, Xiaodong, Surinder Singh, Akhil Garg, Harpreet Singh, Biranchi Panda, Xiongbin Peng and Qiujuan Zhang. "Review of materials used in laser-aided additive manufacturing processes to produce metallic products." *Frontiers of Mechanical Engineering* 14 (2019): 282-298. <https://doi.org/10.1007/s11465-019-0526-1>
- [10] Özen, Arda, Bilen Emek Abali, Christina Völlmecke, Jonathan Gerstel and Dietmar Auhl. "Exploring the role of manufacturing parameters on microstructure and mechanical properties in fused deposition modeling (FDM) using PETG." *Applied Composite Materials* 28, no. 6 (2021): 1799-1828. <https://doi.org/10.1007/s10443-021-09940-9>
- [11] Sheoran, Ankita Jaisingh and Harish Kumar. "Fused Deposition modeling process parameters optimization and effect on mechanical properties and part quality: Review and reflection on present research." *Materials Today: Proceedings* 21 (2020): 1659-1672. <https://doi.org/10.1016/j.matpr.2019.11.296>
- [12] Selvamani, S. K., W. K. Ngui, K. Rajan, M. Samykan, Reji Kumar and Avinash M. Badadhe. "Investigation of bending and compression properties on PLA-brass composite using FDM." *Physics and Chemistry of the Earth, Parts A/B/C* 128 (2022): 103251. <https://doi.org/10.1016/j.pce.2022.103251>
- [13] Samykan, M., S. K. Selvamani, K. Kadirgama, W. K. Ngui, G. Kanagaraj and K. J. T. I. J. O. A. M. T. Sudhakar. "Mechanical property of FDM printed ABS: influence of printing parameters." *The International Journal of Advanced Manufacturing Technology* 102 (2019): 2779-2796. <https://doi.org/10.1007/s00170-019-03313-0>
- [14] Wang, Qianqian, Chencheng Ji, Lushan Sun, Jianzhong Sun and Jun Liu. "Cellulose nanofibrils filled poly (lactic acid) biocomposite filament for FDM 3D printing." *Molecules* 25, no. 10 (2020): 2319. <https://doi.org/10.3390/molecules25102319>
- [15] Ivanov, Evgeni, Rumiana Kotsilkova, Hesheng Xia, Yinghong Chen, Ricardo K. Donato, Katarzyna Donato, Anna Paula Godoy *et al.*, "PLA/Graphene/MWCNT composites with improved electrical and thermal properties suitable for FDM 3D printing applications." *Applied Sciences* 9, no. 6 (2019): 1209. <https://doi.org/10.3390/app9061209>
- [16] Li, Jinhua, Chengtie Wu, Paul K. Chu and Michael Gelinsky. "3D printing of hydrogels: Rational design strategies and emerging biomedical applications." *Materials Science and Engineering: R: Reports* 140 (2020): 100543. <https://doi.org/10.1016/j.mser.2020.100543>

- [17] Kain, Stefan, J. V. Ecker, A. Haider, M. Musso and A. Petutschnigg. "Effects of the infill pattern on mechanical properties of fused layer modeling (FLM) 3D printed wood/polylactic acid (PLA) composites." *European journal of wood and wood products* 78 (2020): 65-74. <https://doi.org/10.1007/s00107-019-01473-0>
- [18] Sun, Q., G. M. Rizvi, C. T. Bellehumeur and P. Gu. "Effect of processing conditions on the bonding quality of FDM polymer filaments." *Rapid prototyping journal* 14, no. 2 (2008): 72-80. <https://doi.org/10.1108/13552540810862028>
- [19] Yang, Leipeng, Shujuan Li, Xing Zhou, Jia Liu, Yan Li, Mingshun Yang, Qilong Yuan and Wei Zhang. "Effects of carbon nanotube on the thermal, mechanical and electrical properties of PLA/CNT printed parts in the FDM process." *Synthetic Metals* 253 (2019): 122-130. <https://doi.org/10.1016/j.synthmet.2019.05.008>
- [20] Luo, Jinjie, Haibao Wang, Duquan Zuo, Anping Ji and Yaowen Liu. "Research on the application of MWCNTs/PLA composite material in the manufacturing of conductive composite products in 3D printing." *Micromachines* 9, no. 12 (2018): 635. <https://doi.org/10.3390/mi9120635>